Utilizing Nonlinear Active Vibration Control to Quench the Nonlinear Vibrations of Helicopter Blade Flapping System

Y. S. HAMED[ID][1,2], **HANAN K. ALKHATHAMI**[3], **AND E. R. EL-ZAHAR**[ID][4,5]

[1]Department of Mathematics and Statistics, College of Science, Taif University, Taif 21944, Saudi Arabia
[2]Department of Physics and Engineering Mathematics, Faculty of Electronic Engineering, Menoufia University, Menouf 32952, Egypt
[3]Department of Mathematics, Faculty of Science, Bisha University, Bisha 61922, Saudi Arabia
[4]Department of Mathematics, College of Sciences and Humanities in Al-Kharj, Prince Sattam bin Abdulaziz University, Al-Kharj 11942, Saudi Arabia
[5]Department of Basic Engineering Science, Faculty of Engineering, Menoufia University, Shebin El-Kom 32511, Egypt

Corresponding author: Y. S. Hamed (yasersalah@tu.edu.sa; eng_yaser_salah@yahoo.com)

ABSTRACT This article utilizes a nonlinear active vibration control to eliminate the helicopter blade flapping system oscillations having mixed excitation forces. The approximate solutions were calculated using the multiple scale perturbation technique. Furthermore, the stability and bifurcation analysis were investigated using the averaging method and Poincaré maps. In addition, numerical results exhibit the amplitude of the steady state against the detuning parameter and, the influences of all the parameters on the vibrating system behavior. Comparisons were carried out between analytical and numerical simulations to enclose the accuracy of our results. Finally, the current work is examined and compared to the published works.

INDEX TERMS Helicopter blade flapping system, active vibration control, vibration, stability.

I. INTRODUCTION

Active vibration control is a widely performed method for controlling the helicopter vibrations. In fact, the helicopter vibrations cannot be completely eliminated, so the active vibration control is essential to minimize the harmful effects and ensure operation safety. Active vibration control to suppress the oscillations of the helicopter's rotor blade has been examined and studied [1]–[3]. The vibrations of an aircraft wing and the phenomenon of saturation suppressing these vibrations have been studied mathematically in resonance cases [4]. An active nonlinear vibration control has been applied to reduce the vibration of the plant at primary excitation and 2:1 internal resonance [5]. The nonlinear saturation control approach reducing vibration of self-excitation of a van der Pol oscillator at 2:1 internal resonance was demonstrated [6]. The behavior of the system with multi types of excitation has been analyzed using passive control approach [7]–[9]. Others have examined the nonlinear behavior and stability analyses for the inclined cable, string beam,

The associate editor coordinating the review of this manuscript and approving it for publication was Guangdeng Zong[ID].

and coupled pitch roll ship system under multiple harmonic and parametric excitations [10]–[12]. To eliminate the rotor blade flapping vibration, the active saturation control has been applied in the presence of 1:1, 1:2 and 1:3 internal resonance with external and parametric excitations [13], [14]. The different types of control to suppress the flexible composite beam vibrations were investigated [15]. The vibration control of the helicopter blade flapping was examined using time delay positive position feedback controller. In addition, the approximate solutions, stability, effects of parameters and effectiveness of the controller were studied [16]. The periodic motion was examined and two different methods calculating the harmonics helicopter blades movement were analyzed and compared [17]. The mathematical approach presented a development for the modelling and analyzed the characteristics of coupled flap-lag torsion vibration of rotor blades. This approach estimated the vibration of first seven coupled modes and showed excellent numerical stability [18]. The process of energy transfer in articulated helicopter rotor blades was presented based on the dynamical coupling existing between the blades and flap/lag modes. Additionally, the stability of these modes was studied using the Poincare map method [19].

The helicopter dynamic model used the vibrations of the fuselage to accelerate the main rotor. PID controllers (proportional, integral, derivative) and Fourier transform processing were used to analyze the behavior of rotor vibrations [20]. Efficient calculations were developed for the dynamic analysis of non-hingeless rotating helicopter blades applying a modified Adomian decomposition method [21]. The control algorithm was investigated in civil structures subject to earthquake excitation. The control algorithm is effective in reducing the response of building structures [22]. The acoustic behavior of vehicle engines has been improved applying the passive methods as well as active ones [23]. The Abaqus application of the newly developed three-node piezoelectric shell element was studied and briefly presented with results of several test cases computed with the component implemented in Abaqus [24]. The energy transfer, bifurcation and stability analyses using Poincare maps and averaging method technique for the MEMS gyroscope and Cartesian manipulator system have been discussed [25], [26]. Active vibration control and nonlinear modified positive position feedback to eliminate the vibrations of cantilever beam and electromechanical oscillator were applied [27], [28]. The different parameters effect, energy transfer and stability were analyzed for the wind turbine system. In addition, the proportional derivative controller to reduce the oscillations was applied [29]. A nonlinear vibrations suppression and energy transfer were investigated for the vertical conveyor system utilizing the proportional derivative controller [30]. Moreover, the analysis of nonlinear vibrations for some dynamical systems was founded in the books [31]–[34]. In this work, the nonlinear active vibration control for suppression the oscillations of helicopter blade flapping system was investigated. In addition, the approximate solutions were calculated using the multiple scale perturbation technique. Furthermore, the stability, bifurcation analysis, numerical simulations for the vibrating system were studied and discussed.

II. EQUATIONS OF THE SYSTEM MOTION

The partial differential equations governing the helicopter blade flapping motion have been derived in detail in [13], [14], [16]. They were discretized by a one-term Galerkin's procedure to have the ordinary differential equations governing the x_1 and x_2 displacements of the helicopter blade. These extracted equations of motion described by a two-degree-of-freedom system and written as follows

$$\ddot{x}_1 + 2\varepsilon\omega_1\zeta_1\dot{x}_1 + \omega_1^2 x_1 + \varepsilon\alpha_1 x_1^3 = \varepsilon f_1 \cos\Omega t$$
$$+ \varepsilon f_2 x_1 \cos\Omega_1 t + \varepsilon f_3 \cos\Omega_2 t \sin\Omega_3 t$$
$$+ \varepsilon\beta_1 x_1(\dot{x}_2)^2 \tag{1}$$
$$\ddot{x}_2 + 2\varepsilon\omega_2\zeta_2\dot{x}_2 + \omega_2^2 x_2 = \varepsilon\beta_2 x_2^2 \dot{x}_1 \tag{2}$$

where x_1 and x_2 are displacement. $\dot{x}_n$, $\ddot{x}_n$ (n = 1, 2) are the first and second derivatives, ζ_1 and ζ_2 are linear damping coefficients, α_1 is non-linear parameter, ε is a small perturbation f_j (j = 1, 2, 3) are the excitation amplitudes, ω_1, ω_2 are the natural frequencies, Ω, Ω_j (j = 1, 2, 3) are excitation frequencies, β_1 and β_2 are active control coefficients.

III. MATHEMATICAL ANALYSIS
To obtain the approximate solutions for the vibrating system, we applied the multiple scale perturbation method [33], [34].

A. PERTURBATION ANALYSIS
The methods of perturbation aim to find approximate analytical solutions to problems whose exact solutions cannot be found. Perturbation methods are designed to construct solutions to a family of equations $p(\varepsilon)$ depending on a parameter $\varepsilon \ll 1$, by adding small corrections to known solutions of $p(0)$. In the solution process of the perturbation problem thereafter, the resulting additional freedom introduced by the new independent variables is used to eliminate (unwanted) secular terms. The latter puts constraints on the approximate solution, which are called solvability conditions. The method of multi-scale perturbation is performed to get the approximate solution of equations (1) and (2). We suppose the solution in the form:

$$\left.\begin{array}{l} x_1(t;\varepsilon) = x_{10}(T_0, T_1) + \varepsilon x_{11}(T_0, T_1) \\ x_2(t;\varepsilon) = x_{20}(T_0, T_1) + \varepsilon x_{21}(T_0, T_1) \end{array}\right\} \tag{3}$$

where T_0 is a fast time scale characterizing motion and $T_1 = \varepsilon t$ is a slow time scale. The time derivatives are given by:

$$\left.\begin{array}{l} \dfrac{d}{dt} = D_0 + \varepsilon D_1 \\ \dfrac{d^2}{dt^2} = D_0^2 + 2\varepsilon D_0 D_1 \end{array}\right\} \tag{4}$$

where $D_0 = \frac{\partial}{\partial T_0}$ and $D_1 = \frac{\partial}{\partial T_1}$

Inserting equations (3) and (4) into equations (1) and (2) and, equating the same power coefficients of ε as:

$$\left(D_0^2 + \omega_1^2\right) x_{10} = 0 \tag{5}$$

$$\left(D_0^2 + \omega_2^2\right) x_{20} = 0 \tag{6}$$

$$(D_0^2 + \omega_1^2)x_{11} = -2D_0 D_1 x_{10} - 2\omega_1\zeta_1 D_0 x_{10} - \alpha_1 x_{10}^3$$
$$+ f_1 \cos\Omega t + f_2 x_{10} \cos\Omega_1 t$$
$$+ f_3 \cos\Omega_2 t \sin\Omega_3 t + \beta_1 x_{10}(D_0 x_{20})^2 \tag{7}$$

$$\left(D_0^2 + \omega_2^2\right) x_{21} = -2D_0 D_1 x_{20} - 2\omega_2\zeta_2 D_0 x_{20} + \beta_2 x_{20}^2 D_0 x_{10} \tag{8}$$

The general solutions of equations (5) and (6) have the form:

$$x_{10} = A_0 e^{i\omega_1 T_0} + \overline{A_0} e^{-i\omega_1 T_0} \tag{9}$$
$$x_{20} = B_0 e^{i\omega_2 T_0} + \overline{B_0} e^{-i\omega_2 T_0} \tag{10}$$

where $A_0, \bar{A}_0, B_0$ and $\bar{B}_0$ is complex functions in T_1.

Substituting equations (9) and (10) into equations (7) and (8), and eliminated the secular terms $e^{\pm i\omega_1 T_0}$ and

$e^{\pm i\omega_2 T_0}$, the solution will be in the form

$$
\begin{aligned}
x_{11} =\ & A_1 \exp(i\omega_1 T_0) + \overline{A_1} \exp(-i\omega_1 T_0) \\
& + \frac{\alpha_1}{8\omega_1^2}\left[A_0^3 \exp(3i\omega_1 T_0) + \overline{A_0}^3 \exp(-3i\omega_1 T_0)\right] \\
& + \frac{f_1}{2(\omega_1^2 - \Omega^2)}\left[\exp(i\Omega T_0) + \exp(-i\Omega T_0)\right] \\
& + \frac{f_2 A_0}{2(\omega_1^2 - (\Omega_1 + \omega_1)^2)}\exp(iT_0(\Omega_1 + \omega_1)) \\
& + \frac{f_2 \overline{A_0}}{2(\omega_1^2 - (\Omega_1 + \omega_1)^2)}\exp(-iT_0(\Omega_1 + \omega_1)) \\
& + \frac{f_2 A_0}{2(\omega_1^2 - (\omega_1 - \Omega_1)^2)}\exp(iT_0(\omega_1 - \Omega_1)) \\
& + \frac{f_2 \overline{A_0}}{2(\omega_1^2 - (\Omega_1 - \omega_1)^2)}\exp(-iT_0(\omega_1 - \Omega_1)) \\
& - \frac{if_3}{4(\omega_1^2 - (\Omega_3 + \Omega_2)^2)}\exp(iT_0(\Omega_3 + \Omega_2)) \\
& + \frac{if_3}{4(\omega_1^2 - (\Omega_3 + \Omega_2)^2)}\exp(-iT_0(\Omega_3 + \Omega_2)) \\
& - \frac{if_3}{4(\omega_1^2 - (\Omega_3 - \Omega_2)^2)}\exp(iT_0(\Omega_3 - \Omega_2)) \\
& + \frac{if_3}{4(\omega_1^2 - (\Omega_2 - \Omega_3)^2)}\exp(-iT_0(\Omega_3 - \Omega_2)) \\
& - \frac{\beta_1 B_0^2 A_0 \omega_2^2}{(\omega_1^2 - (2\omega_2 + \omega_1)^2)}\exp(iT_0(\omega_1 + 2\omega_2)) \\
& - \frac{\beta_1 \overline{B_0}^2 \overline{A_0} \omega_2^2}{(\omega_1^2 - (\omega_1 + 2\omega_2)^2)}\exp(-iT_0(\omega_1 + 2\omega_2)) \\
& - \frac{\beta_1 \overline{B_0}^2 A_0 \omega_2^2}{(\omega_1^2 - (\omega_1 - 2\omega_2)^2)}\exp(iT_0(\omega_1 - 2\omega_2)) \\
& - \frac{\beta_1 B_0^2 \overline{A_0} \omega_2^2}{(\omega_1^2 - (2\omega_2 - \omega_1)^2)}\exp(-iT_0(\omega_1 - 2\omega_2)) \quad (11)
\end{aligned}
$$

$$
\begin{aligned}
x_{21} =\ & B_1 \exp(i\omega_2 T_0) + \overline{B_1} \exp(-i\omega_2 T_0) \\
& + \frac{i\omega_1 \beta_2 B_0^2 A_0}{(\omega_2^2 - (2\omega_2 + \omega_1)^2)}\exp(iT_0(2\omega_2 + \omega_1)) \\
& - \frac{i\omega_1 \beta_2 \overline{B_0}^2 \overline{A_0}}{(\omega_2^2 - (2\omega_2 + \omega_1)^2)}\exp(-iT_0(2\omega_2 + \omega_1)) \\
& - \frac{i\omega_1 \beta_2 B_0^2 \overline{A_0}}{(\omega_2^2 - (2\omega_2 - \omega_1)^2)}\exp(iT_0(2\omega_2 - \omega_1)) \\
& + \frac{i\omega_1 \beta_2 \overline{B_0}^2 A_0}{(\omega_2^2 - (\omega_1 - 2\omega_2)^2)}\exp(-iT_0(2\omega_2 - \omega_1)) \\
& + \frac{2i\omega_1 \beta_2 B_0 \overline{B_0} A_0}{(\omega_2^2 - \omega_1^2)}\exp(i\omega_1 T_0) \\
& - \frac{2i\omega_1 \beta_2 \overline{B_0} B_0 \overline{A_0}}{(\omega_2^2 - \omega_1^2)}\exp(-i\omega_1 T_0) \quad (12)
\end{aligned}
$$

where $A_1, \bar{A}_1, B_1$ and $\bar{B}_1$ is complex functions in T_1.

B. AVERAGING METHOD

The frequency response equations for equations (1) and (2) using the averaging method [26], [27] is utilized. When $\varepsilon = 0$, the general solution of equations (1) and (2) can be expressed as:

$$x_1 = a\cos(\omega_1 t + \psi) \quad (13)$$
$$x_2 = b\cos(\omega_2 t + \phi) \quad (14)$$

where a, b, ψ and ϕ are constants. It follows from equations (13) and (14) that

$$\dot{x}_1 = -\omega_1 a \sin(\omega_1 t + \psi) \quad (15)$$
$$\dot{x}_2 = -\omega_2 b \sin(\omega_2 t + \phi) \quad (16)$$

For $\varepsilon \neq 0$ small enough, let a, b, ψ and ϕ are functions in t, and differentiate the equations (13) and (14) with respect to t, we gets

$$
\begin{aligned}
\dot{x}_1 =\ & \dot{a}\cos(\omega_1 t + \psi) - \omega_1 a \sin(\omega_1 t + \psi) \\
& - a_1 \dot{\psi}\sin(\omega_1 t + \psi) \quad (17) \\
\dot{x}_2 =\ & \dot{b}\cos(\omega_2 t + \phi) - \omega_2 b \sin(\omega_2 t + \phi) \\
& - b\dot{\phi}\sin(\omega_2 t + \phi) \quad (18)
\end{aligned}
$$

Comparing equations (15) and (16) with (17) and (18), we conclude that

$$\dot{a}\cos(\omega_1 t + \psi) - a\dot{\psi}\sin(\omega_1 t + \psi) = 0 \quad (19)$$
$$\dot{b}\cos(\omega_2 t + \phi) - b\dot{\phi}\sin(\omega_2 t + \phi) = 0 \quad (20)$$

Differentiate the equations (15) and (16) with respect to t, we have

$$
\begin{aligned}
\ddot{x}_1 =\ & -\omega_1 \dot{a}\sin(\omega_1 t + \psi) - \omega_1^2 a \cos(\omega_1 t + \psi) \\
& - \omega_1 a\dot{\psi}\cos(\omega_1 t + \psi) \quad (21) \\
\ddot{x}_2 =\ & -\omega_2 \dot{b}\sin(\omega_2 t + \phi) - \omega_2^2 b \cos(\omega_2 t + \phi) \\
& - \omega_2 b\dot{\phi}\cos(\omega_2 t + \phi) \quad (22)
\end{aligned}
$$

Inserting for $x_1, x_2, \dot{x}_1, \dot{x}_2, \ddot{x}_1$ and $\ddot{x}_2$ from equations (13)-(22) into equations (1) and (2), we obtain

$$
\begin{aligned}
& \dot{a}\sin(\omega_1 t + \psi) + a\dot{\psi}\cos(\omega_1 t + \psi) \\
& \quad + 2\varepsilon a\omega_1 \zeta_1 \sin(\omega_1 t + \psi) - \frac{\varepsilon\alpha_1 a^3}{\omega_1}\cos^3(\omega_1 t + \psi) \\
& = -\frac{\varepsilon f_1}{\omega_1}\cos\Omega t - \frac{\varepsilon a f_2}{\omega_1}\cos(\omega_1 t + \psi)\cos\Omega_1 t - \frac{\varepsilon f_3}{\omega_1}\cos\Omega_2 t \\
& \quad \times \sin\Omega_3 t - \frac{\varepsilon\beta_1 ab^2\omega_2^2}{\omega_1}\cos(\omega_1 t + \psi)\sin^2(\omega_2 t + \phi) \quad (23) \\
& \dot{b}\sin(\omega_2 t + \phi) + b\dot{\phi}\cos(\omega_2 t + \phi) + 2\varepsilon\omega_2 \zeta_2 b \sin(\omega_2 t + \phi) \\
& = \frac{\varepsilon\beta_2 ab^2\omega_1}{\omega_2}\cos^2(\omega_2 t + \phi)\sin(\omega_1 t + \psi) \quad (24)
\end{aligned}
$$

Inserting equations (19), (20) into equations (23), (24) and solving it for a, b, ψ and ϕ yield

$$
\begin{aligned}
& \dot{a} + \varepsilon a\omega_1 \zeta_1 \left[1 - \cos(2\omega_1 t + 2\psi)\right] \\
& \quad - \frac{\varepsilon\alpha_1 a^3}{\omega_1}\left[\frac{1}{8}\sin(4\omega_1 t + 4\psi) + \frac{1}{4}\sin(2\omega_1 t + 2\psi)\right]
\end{aligned}
$$

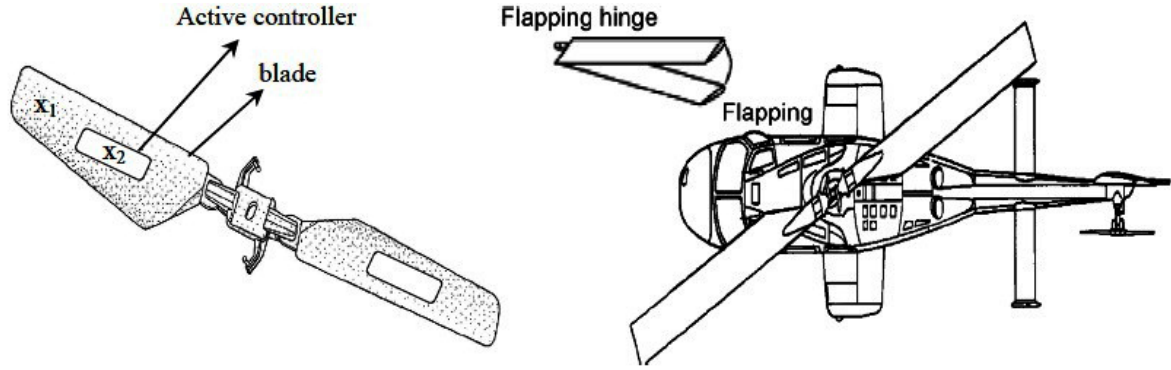**FIGURE 1.** Schematic diagram of the helicopter blade flapping [13], [14], [16].

$$= -\frac{\varepsilon f_1}{2\omega_1}[\sin((\Omega + \omega_1)t + \psi) - \sin((\Omega - \omega_1)t - \psi)]$$
$$- \frac{\varepsilon a f_2}{4\omega_1}[\sin((\Omega_1 + 2\omega_1)t + 2\psi) - \sin((\Omega_1 - 2\omega_1)t - 2\psi)]$$
$$- \frac{\varepsilon f_3}{4\omega_1}[\cos((\Omega_2 - \Omega_3 + \omega_1)t + \psi)$$
$$- \cos((\Omega_2 - \Omega_3 - \omega_1)t - \psi)$$
$$+ \cos((\Omega_2 + \Omega_3 - \omega_1)t - \psi) - \cos((\Omega_2 + \Omega_3 + \omega_1)t + \psi)]$$
$$- \frac{\varepsilon\beta_1 ab^2 \omega_2^2}{4\omega_1}[\sin(2\omega_1 t + 2\psi) - \sin((2\omega_1 + 2\omega_2)t + 2\psi$$
$$+ 2\phi) + \sin((2\omega_2 - 2\omega_1)t + 2\phi - 2\psi)] \quad (25)$$

$$a\dot\psi + \varepsilon a\omega_1\zeta_1 \sin(2\omega_1 t + 2\psi) - \frac{\varepsilon a f_2}{2\omega_1}[\cos\Omega_1 t$$
$$+ \frac{1}{2}\cos((\Omega_1 + 2\omega_1)t + 2\psi) + \frac{1}{2}\cos((\Omega_1 - 2\omega_1)t - 2\psi)]$$
$$- \frac{\varepsilon\alpha_1 a^3}{\omega_1}\left[\frac{3}{8} + \frac{1}{8}\cos(4\omega_1 t + 4\psi) + \frac{1}{2}\cos(2\omega_1 t + 2\psi)\right]$$
$$= -\frac{\varepsilon f_1}{2\omega_1}[\cos((\Omega + \omega_1)t + \psi) + \cos((\Omega - \omega_1)t - \psi)]$$
$$- \frac{\varepsilon f_3}{4\omega_1}[\sin((\Omega_2 + \Omega_3 + \omega_1)t + \psi)$$
$$+ \sin((\Omega_2 + \Omega_3 - \omega_1)t - \psi)$$
$$- \sin((\Omega_2 - \Omega_3 - \omega_1)t - \psi) - \sin((\Omega_2 - \Omega_3 + \omega_1)t + \psi)]$$
$$- \frac{\varepsilon\beta_1 ab^2 \omega_2^2}{4\omega_1}[1 - \cos(2\omega_2 t + 2\phi) + \cos(2\omega_1 t + 2\psi)$$
$$- \frac{1}{2}\cos((2\omega_1 + 2\omega_2)t + 2\psi + 2\phi)$$
$$- \frac{1}{2}\cos((2\omega_2 - 2\omega_1)t + 2\phi - 2\psi)] \quad (26)$$

$$b\dot\phi + \varepsilon b\omega_2\zeta_2 \sin(2\omega_1 t + 2\psi)$$
$$= \frac{\varepsilon\beta_1 ab^2 \omega_2^2}{4\omega_1}[3\sin((\omega_1 + \omega_2)t + \psi + \phi)$$
$$- \cos((\omega_1 + 3\omega_2)t + 3\phi + \psi)] \quad (27)$$

$$\dot b + \varepsilon b\omega_2\zeta_2 [1 - \cos(2\omega_2 t + 2\phi)]$$
$$= \frac{\varepsilon\beta_2 ab^2 \omega_1}{8\omega_2}[-\cos((\omega_1 + \omega_2)t + \phi + \psi) + \cos((\omega_1 - \omega_2)t$$
$$+ \psi - \phi) + \cos((\omega_1 - 3\omega_2)t + \psi - 3\phi)$$

$$+ 3\sin((\omega_1 - \omega_2)t + \psi - \phi)] + \sin((\omega_1$$
$$+ 3\omega_2)t + \psi + 3\phi) + \sin((\omega_1 - 3\omega_2)t + \psi - 3\phi) \quad (28)$$

C. PERIODIC SOLUTIONS
In this section, the averaging equations is obtained at primary, sub-harmonic, combined and 1:3 internal resonance utilizing the detuning parameters $(\sigma_1, \sigma_2, \sigma_3, \sigma_4)$ as $(\Omega = \omega_1 + \varepsilon\sigma_1, \Omega_1 - \omega_1 = \omega_1 + \varepsilon\sigma_2, \Omega_2 - \Omega_3 = \omega_1 + \varepsilon\sigma_3, 3\omega_2 = \omega_1 + \varepsilon\sigma_4)$ and keeping only the slowly varying parts and constant terms in equations (25)-(28), we have

$$\dot a = -a\omega_1\zeta_1 + \frac{f_1}{2\omega_1}\sin\theta_1 + \frac{f_2 a}{4\omega_1}\sin\theta_2 + \frac{f_3}{4\omega_1}\cos\theta_3$$

$$a\dot\psi = \frac{3\alpha_1 a^3}{8\omega_1} - \frac{\omega_2^2\beta_1 ab^2}{4\omega_1} - \frac{f_1}{2\omega_1}\cos\theta_1 - \frac{f_2 a}{4\omega_1}\cos\theta_2 \quad (29)$$
$$+ \frac{f_3}{4\omega_1}\sin\theta_3 \quad (30)$$

$$\dot b = -b\omega_2\zeta_2 + \frac{\omega_1\beta_2 ab^2}{8\omega_2}\cos\theta_4 \quad (31)$$

$$b\dot\phi = \frac{\omega_1\beta_2 ab^2}{8\omega_2}\sin\theta_4 \quad (32)$$

where $\theta_1 = \sigma_1 T_1 - \psi$, $\theta_2 = \sigma_2 T_1 - 2\psi$, $\theta_3 = \sigma_3 T_1 - \psi$, $\theta_4 = \psi - 3\phi - \sigma_4 T_1$, and $\sigma_1 = \frac{\sigma_2}{2} = \sigma$

D. STABILITY ANALYSES AND EQUILIBRIUM SOLUTIONS
The fixed point of the equations (29)–(32) is obtained when $\dot a = 0, \dot b = 0$, and $\dot\theta_n = 0$, where (n = 1, 4) as the following

$$a\omega_1\zeta_1 = \frac{f_1}{2\omega_1}\sin\theta_1 + \frac{f_2 a}{4\omega_1}\sin\theta_2 + \frac{f_3}{4\omega_1}\cos\theta_3 \quad (33)$$

$$a\sigma - \frac{3\alpha_1 a^3}{8\omega_1} + \frac{\omega_2^2\beta_1 ab^2}{4\omega_1}$$
$$= -\frac{f_1}{2\omega_1}\cos\theta_1 - \frac{f_2 a}{4\omega_1}\cos\theta_2 + \frac{f_3}{4\omega_1}\sin\theta_3 \quad (34)$$

$$b\omega_2\zeta_2 = \frac{\omega_1\beta_2 ab^2}{8\omega_2}\cos\theta_4 \quad (35)$$

$$b\frac{(\sigma - \sigma_4)}{3} = \frac{\omega_1\beta_2 ab^2}{8\omega_2}\sin\theta_4 \quad (36)$$

TABLE 1. Summary of the different worst resonance cases of the system.

Case	Condition	Amplitude x_1 without controller	Amplitude x_1 With controller	E_a
$\Omega = \omega_1, \Omega_1 = 2\omega_1, \Omega_2 - \Omega_3 = \omega_1$	$\omega_1 = 3\omega_2$	0.45	0.011	40
$\Omega = \omega_1, \Omega_1 = \omega_1, \Omega_2 - \Omega_3 = \omega_1$	$\omega_1 = 3\omega_2$	0.44	0.012	36
$\Omega = \omega_1, \Omega_1 = 4\omega_1, \Omega_2 - \Omega_3 = \omega_1$	$\omega_1 = 3\omega_2$	0.44	0.015	29
$\Omega = \omega_1, \Omega_1 = 2\omega_1, \Omega_2 - \Omega_3 = 3\omega_1$	$\omega_1 = 3\omega_2$	0.45	0.013	34
$\Omega = \omega_1, \Omega_1 = \omega_1, \Omega_2 - \Omega_3 = 3\omega_1$	$\omega_1 = 3\omega_2$	0.44	0.014%	31
$\Omega = \omega_1, \Omega_1 = 4\omega_1, \Omega_2 - \Omega_3 = 3\omega_1$	$\omega_1 = 3\omega_2$	0.44	0.015%	30

For practical case ($a \neq 0, b \neq 0$), we obtain the frequency response equations as:

$$\sigma^2 + \left[\frac{\omega_2^2 \beta_1 b^2}{2\omega_1} - \frac{3\alpha_1 a^2}{4\omega_1} \right] \sigma + \omega_1^2 \zeta_1^2 + \frac{9\alpha_1^2 a^4}{64\omega_1^2} + \frac{\omega_2^4 \beta_1^2 b^4}{16\omega_1^2}$$

$$- \frac{3\omega_2^2 \beta_1 \alpha_1 a^2 b^2}{16\omega_1^2} - \frac{f_1^2}{4\omega_1^2 a^2} - \frac{f_2^2}{16\omega_1^2} - \frac{f_3^2}{16\omega_1^2 a^2}$$

$$- \frac{f_1 f_2}{4\omega_1^2 a} \cos(\theta_1 - \theta_2) - \frac{f_1 f_3}{4\omega_1^2 a^2} \sin(\theta_1 - \theta_3)$$

$$- \frac{f_2 f_3}{8\omega_1^2 a} \sin(\theta_2 - \theta_3) = 0 \qquad (37)$$

$$\sigma_4^2 - 2\sigma\sigma_4 + \left[\sigma^2 + 9\omega_2^2 \zeta_2^2 - \frac{9\omega_1^2 a^2 b^2 \beta_2^2}{64\omega_2^2} \right] = 0 \qquad (38)$$

To discuss the stability of the nonlinear solution, we lets

$$a = a_0 + a_1(T_1), \quad b = b_0 + b_1(T_1), \quad \theta_n$$
$$= \theta_{n0} + \theta_{n1}(T_1); \quad n = 1, 4 \qquad (39)$$

where a_0, b_0 and θ_{n0} are the solutions of (29)–(32). Inserting (39) into (29)–(32) and linearizing equations in a_1, b_1 and θ_{n1}, we get

$$\dot{a}_1 = \left(\frac{f_2}{4\omega_1} \sin 2\theta_{10} - \omega_1 \zeta_1 \right) a_1 + \left(\frac{f_1}{2\omega_1} \cos \theta_{10} \right.$$
$$\left. + \frac{a_0 f_2}{2\omega_1} \cos 2\theta_{10} - \frac{f_3}{4\omega_1} \sin \theta_{10} \right) \theta_{11} \qquad (40)$$

$$\dot{\theta}_{11} = \left(\frac{\sigma}{a_0} - \frac{9\alpha_1 a_0}{8\omega_1} + \frac{\omega_2^2 \beta_1 b_0^2}{4\omega_1 a_0} + \frac{f_2}{4\omega_1 a_0} \cos 2\theta_{10} \right) a_1$$
$$+ \left(-\frac{f_1}{2\omega_1 a_0} \sin \theta_{10} - \frac{f_2}{2\omega_1} \sin 2\theta_{10} \right.$$
$$\left. - \frac{f_3}{4\omega_1 a_0} \cos \theta_{10} \right) \theta_{11} + \left(\frac{\omega_2^2 \beta_1 b_0}{2\omega_1} \right) b_1 \qquad (41)$$

$$\dot{b}_1 = \left(\frac{\omega_1 \beta_2 b_0^2}{8\omega_2} \cos \theta_{40} \right) a_1 + \left(-\omega_2 \zeta_2 + \frac{\omega_1 \beta_2 a_0 b_0}{4\omega_2} \cos \theta_{40} \right) b_1$$
$$+ \left(-\frac{\omega_1 \beta_2 a_0 b_0^2}{8\omega_2} \sin \theta_{40} \right) \theta_{41} \qquad (42)$$

$$\dot{\theta}_{41} = \left(-\frac{\sigma_4}{a_0} + \frac{9\alpha_1 a_0}{8\omega_1} - \frac{\omega_2^2 \beta_1 b_0^2}{4\omega_1 a_0} - \frac{f_2}{4a_0\omega_1} \cos 2\theta_{10} \right.$$
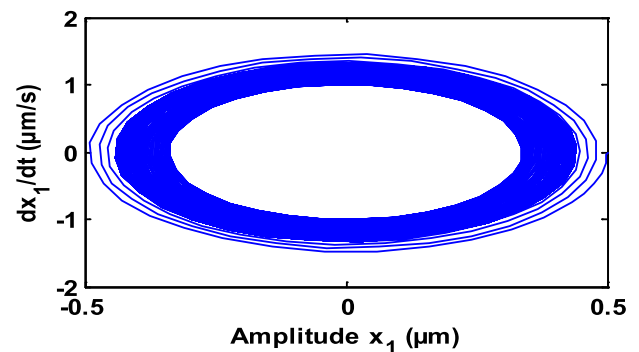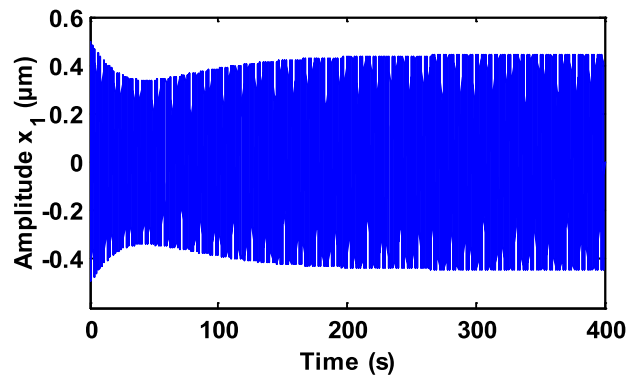
FIGURE 2. System behavior without controller at primary, sub-harmonic and combined resonance case $\Omega = \omega_1, \Omega_1 = 2\omega_1, \Omega_2 - \Omega_3 = \omega_1$.

FIGURE 3. The response of the system and controller at primary, sub-harmonic, combined and internal resonance case $\Omega = \omega_1$, $\Omega_1 = 2\omega_1$, $\Omega_2 - \Omega_3 = \omega_1$, and $3\omega_2 = \omega_1$ at $f_1 = 0.05$, $f_2 = 0.004$, $f_3 = 0.003$ (a) Time history (b) Phase plane (c) Poincare' maps.
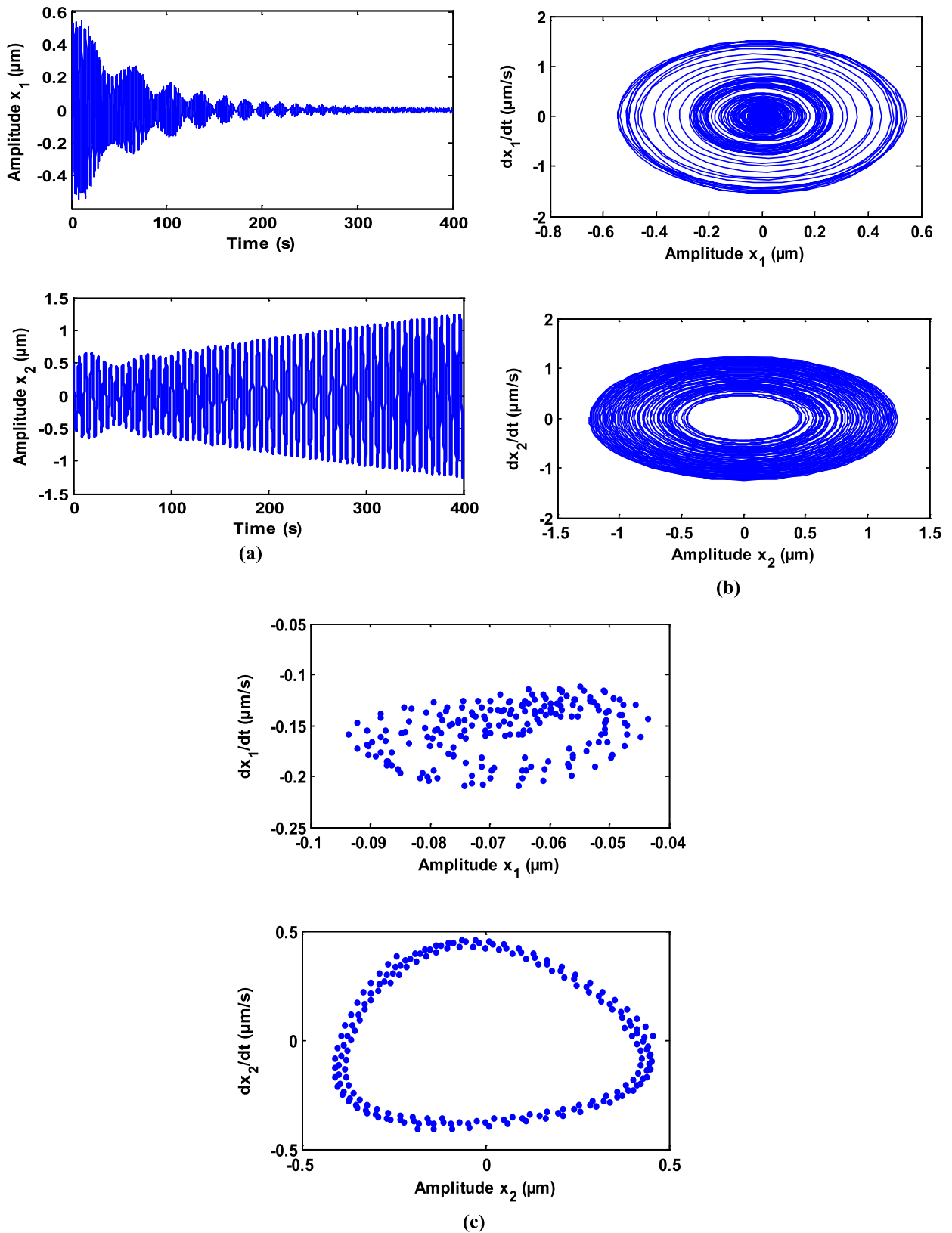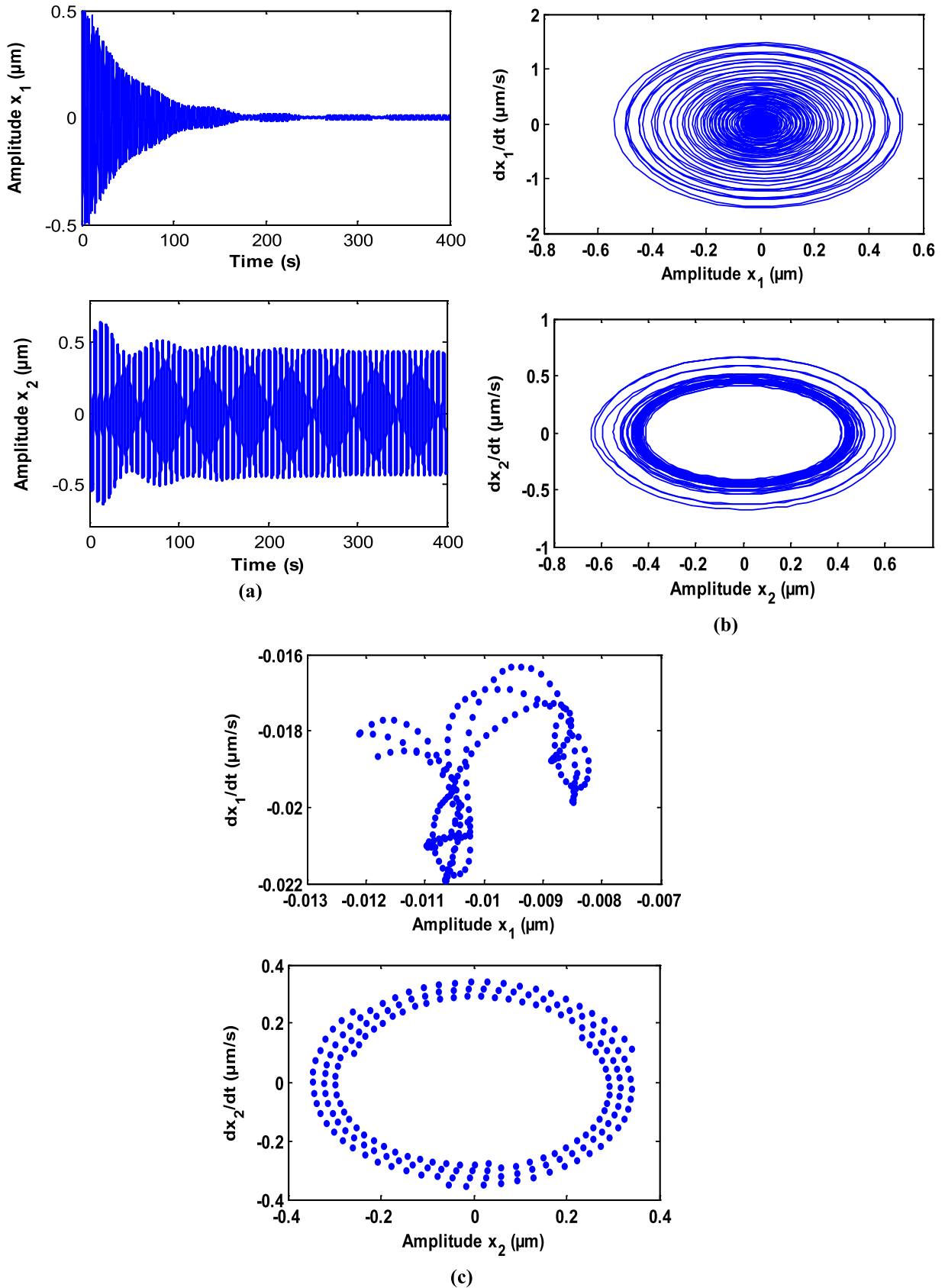
FIGURE 4. The response of the system and controller at primary, sub-harmonic, combined and internal resonance case $\Omega = \omega_1$, $\Omega_1 = 2\omega_1$, $\Omega_2 - \Omega_3 = \omega_1$, and $3\omega_2 = \omega_1$ at $f_1 = 0.005$, $f_2 = 0.0004$, $f_3 = 0.0003$ (a) Time history (b) Phase plane (c) Poincare' maps.

(a) Effects of the detuning parameter σ

(b) Effects of the damping coefficient ζ_1

(c) Effects of the natural frequencies ω_1, ω_2

(d) Effects of the nonlinear parameter

(e) Effects of the nonlinear parameter β_1

(f) Effect of damping coefficient ζ_2 and the nonlinear parameter β_2

(g) Effects of the excitation force amplitude f_1

(h) Effects of the excitation force amplitude f_2

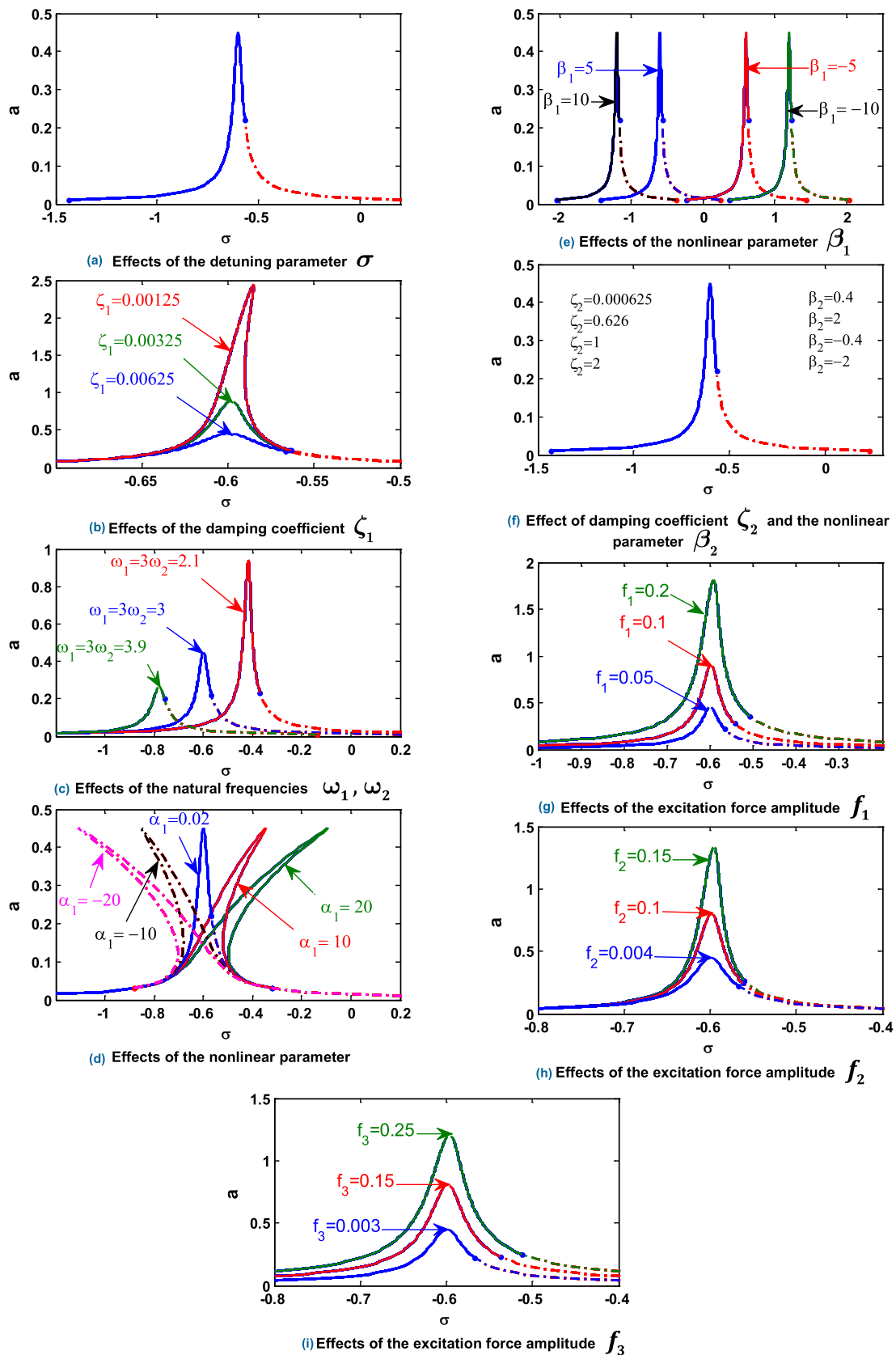(i) Effects of the excitation force amplitude f_3

FIGURE 5. The response curves of the system for different parameters against σ.

TABLE 2. Comparison of results obtained from numerical solution and perturbation solution for the system before and after control the excitation force f_1 as in Fig. 7(a).

f_1	System before control		System after control	
	Numerical Solution	perturbation solution	Numerical Solution	perturbation solution
0	0.01545	0.01543	0.00619	0.00617
0.005	0.04553	0.04550	0.01334	0.01332
0.01	0.0856	0.0854	0.01851	0.01848
0.015	0.1265	0.1263	0.02134	0.02132
0.02	0.1676	0.1674	0.02604	0.02602
0.025	0.2089	0.2086	0.02605	0.02603
0.3	0.2504	0.250	0.02637	0.02634
0.035	0.2919	0.2916	0.02981	0.02977
0.04	0.3335	0.3333	0.02935	0.02933
0.045	0.375	0.3746	0.03198	0.03196
0.05	0.4166	0.4163	0.0347	0.0344

TABLE 3. Comparison of results obtained from numerical solution and perturbation solution for the system before and after control for the control parameter β_1 as in Fig. 7(b).

β_1	System before control		System after control	
	Numerical Solution	perturbation solution	Numerical Solution	perturbation solution
0	0.4166	0.4164	0.167	0.166
0.2	0.4134	0.4133	0.166	0.165
0.2	0.4	0.3994	0.1605	0.1603
0.6	0.3817	0.3814	0.1519	0.1517
0.8	0.3593	0.3591	0.143	0.142
1	0.3366	0.3364	0.1342	0.1340
1.2	0.3147	0.3145	0.1257	0.1256
1.4	0.2938	0.2936	0.1174	0.1173
1.6	0.2739	0.2736	0.1093	0.1091
1.8	0.2557	0.2554	0.102	0.1018
2	0.2397	0.2396	0.09585	0.09583
2.2	0.2254	0.2253	0.09036	0.09035
2.4	0.2121	0.2118	0.08499	0.08497
2.6	0.1996	0.1992	0.07979	0.07977
2.8	0.1884	0.1882	0.07527	0.07526
3	0.1788	0.1786	0.0716	0.0714

$$\left. - \frac{3\omega_1 \beta_2 b_0}{4\omega_2} \sin\theta_{40} \right) a_1 + \left(\frac{f_1}{2a_0\omega_1} \sin\theta_{10} \right.$$

$$+ \frac{f_2}{2\omega_1} \sin 2\theta_{10} + \left. \frac{f_3}{4a_0\omega_1} \cos\theta_{10} \right) \theta_{11}$$

$$+ \left(-\frac{\omega_2^2 \beta_1 b_0}{2\omega_1} - \frac{3\omega_1 \beta_2 a_0}{8\omega_2} \sin\theta_{40} \right) b_1$$

$$- \left(\frac{3\omega_1 \beta_2 a_0 b_0}{8\omega_2} \cos\theta_{40} \right) \theta_{41} \tag{43}$$

The characteristic equation of the system (40)-(43) is a four-degree equation in the form:

$$\lambda^4 + r_1\lambda^3 + r_2\lambda^2 + r_3\lambda + r_4 = 0 \tag{44}$$

where r_1, r_2, r_3 and r_4 are constants and they are given in the Appendix. If the real part of the eigenvalue is negative, the periodic solution is stable, otherwise, it becomes unstable. According to the Routh–Huriwitz criterion, the necessary and sufficient conditions for all roots of (44) to obtain negative

real parts, the following equation is satisfied:

$$r_1 > 0, \quad r_1 r_2 - r_3 > 0, \; r_3\,(r_1 r_2 - r_3) - r_1^2 r_4 > 0, \; r_4 > 0 \tag{45}$$

IV. RESULTS AND DISCUSSION

In this section, we apply Runge-Kutta fourth-order method to achieve the numerical results. The bifurcation diagrams and effect of different parameters on the steady state solution before and after control are reported and discussed. Finally, the comparison of analytical results with numerical ones is investigated. Table 1. Summary of the different worst resonance cases of the system.

A. SYSTEM BEHAVIOR

At the worst resonance cases $\Omega = \omega_1, \Omega_1 = 2\omega_1$ and $\Omega_2 - \Omega_3 = \omega_1$, the system behavior was studied numerically for the equations (1) and (2) at the selected parameters:
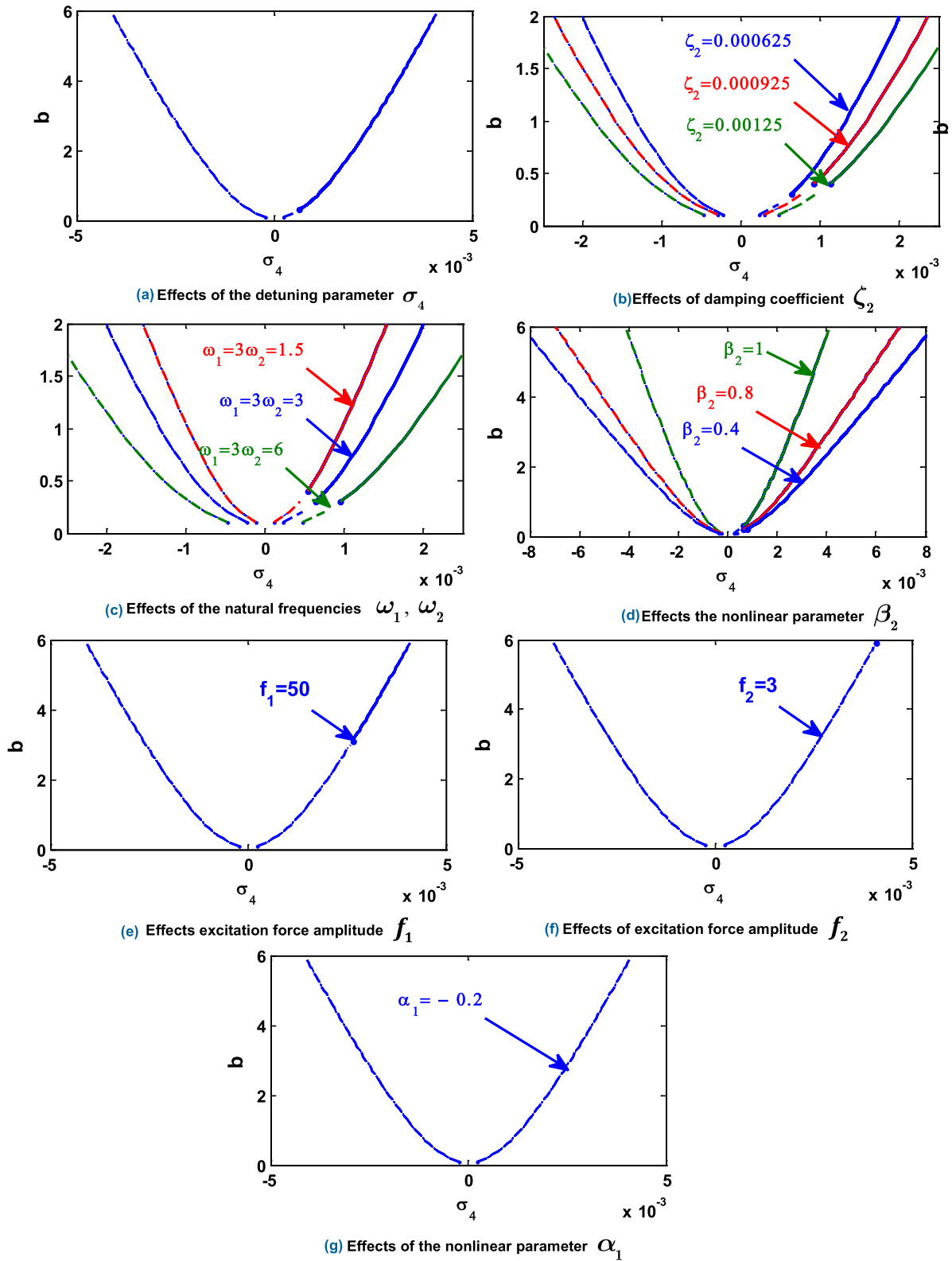
(a) Effects of the detuning parameter σ_4

(b) Effects of damping coefficient ζ_2

(c) Effects of the natural frequencies ω_1, ω_2

(d) Effects the nonlinear parameter β_2

(e) Effects excitation force amplitude f_1

(f) Effects of excitation force amplitude f_2

(g) Effects of the nonlinear parameter α_1

FIGURE 6. The response curves of the controller for different parameters against σ_4.

$\zeta_1 = 0.00625, \zeta_2 = 0.000625, \alpha_1 = 0.02, \beta_1 = 5, \beta_2 = 0.4, f_1 = 0.05, f_2 = 0.004, f_3 = 0.003,$ $\omega_1 = 3, \omega_2 = 1, \Omega = 3, \Omega_1 = 6, \Omega_2 = 4, \Omega_3 = 1.$ Figure 2 illustrates the response and phase plane of the system

without control, with this figure, the response amplitude of the system x_1 is nearly about **0.45** and the phase plane shows limit cycle.

Figure 3 illustrates the response, phase plane and Poincaré maps of the system with control at the resonance case $\Omega = \omega_1, \Omega_1 = 2\omega_1, \Omega_2 - \Omega_3 = \omega_1$, and $3\omega_2 = \omega_1$. It can be seen for the main system that the amplitude x_1 is nearly about **0.011** and the controller reduced the vibrations of the system by about **97.55%** from its value before controllers and the phase plane shows limit cycle and, the efficiency of the controllers E_a is nearly about **40** as shown in figure 3(a, b). Moreover, the system response is chaotic, and the Poincaré maps has a quasi-periodic at $f_1 = 0.05, f_2 = 0.004, f_3 = 0.003$ as shown in figure 3(c).
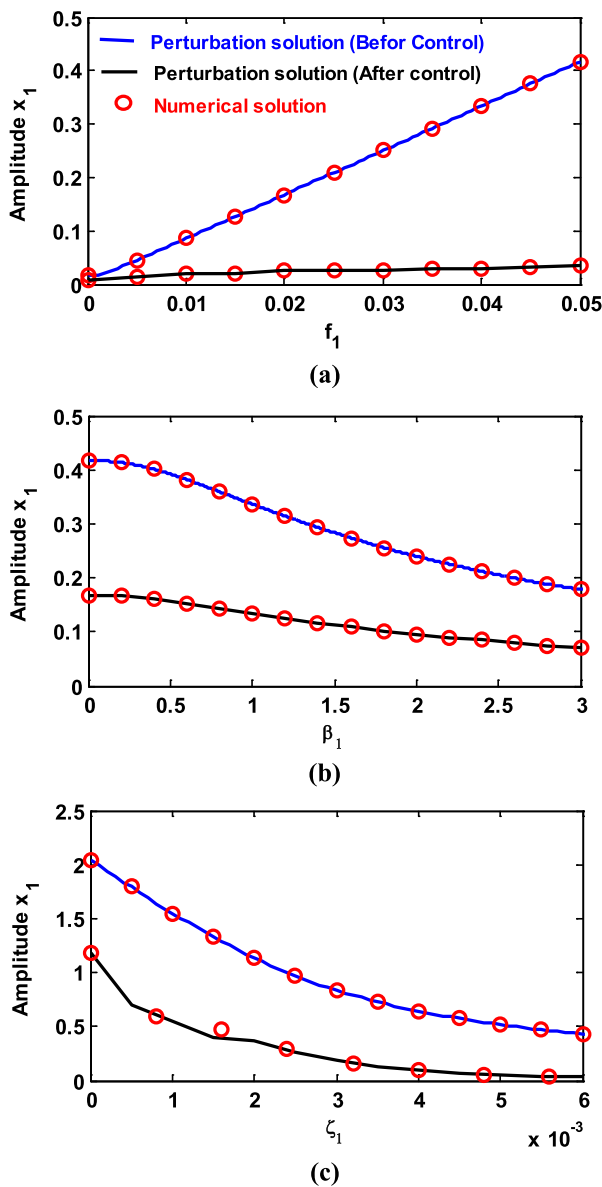
The system amplitude x_1 is nearly about **0.01** and the controller reduced the vibrations of the system by about **97.77%** from its value before controllers and the phase plane has limit cycle and, the efficiency of the controllers E_a is nearly about **45** as shown in figure 4(a, b). Also, the Poincaré maps has a quasi-periodic motion at $f_1 = 0.005, f_2 = 0.0004, f_3 = 0.0003$ as shown in figure 4(c).

B. NUMERICAL RESULTS OF STEADY STATE SOLUTION

With solving equations (37) and (38), the different parameters effects were investigated and the results are shown in Figures (5, 6). From the figures, we have a jump phenomenon with multi-valued solutions for the practical case where $a \neq 0, b \neq 0$. Figure 5(a) indicate the steady state amplitude of the system with the effect of the detuning parameter σ. Figures 5(b, c) show that the amplitude of the system are decreasing functions in the linear damping coefficient ζ_1 and natural frequencies ω_1 and ω_2. The frequency response curves bent to right or to left leading to the jump phenomena and multivalued solution for positive and negative values of the nonlinear parameter α_1 also, the unstable region increases with the negative values of α_1 as shown in figures. 5(d). The frequency response curves are shifted to the left with increasing values of the nonlinear parameter β_1 as shown in figures 5(e). Figure 5(f) shows that the system amplitude has trivial effect with different values of the damping coefficient ζ_2 and nonlinear parameter β_2. Figures 5(g, h, i) show that the amplitude of the system is increased with increasing values of the excitation force amplitudes f_1, f_2 and f_3.

Figure. 6(a) shows the effects of detuning parameter σ_4 on the amplitude of the controller b. Figures 6(b, c) show that the amplitude of the controller are decreasing functions in the linear damping coefficient ζ_2, natural frequencies ω_1 and ω_2. Figure 6(d) shows that the amplitude of the controller is increasing function in the nonlinear parameters β_2. For large excitation force amplitudes f_1, f_2 and negative value nonlinear parameter α_1, the regions of unstable solutions increases as shown in figures 6(e, f, g).

(a)

(b)

(c)

FIGURE 7. Effect of some different parameters on the system before and after control (a) Effects of force f_1 (b) Effects of damping coefficient ζ_1 (c) Effect of the control parameter β_1.
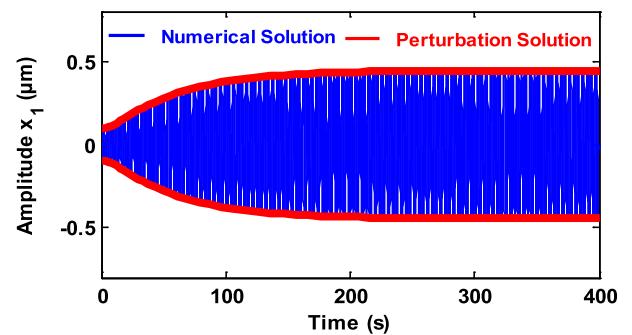
FIGURE 8. Comparison of the numerical solution with the analytical solution of the system before control at $\beta_1 = 0, \beta_2 = 0$ and $x_1(0) = 0.1$, $\dot{x}_1(0) = 0.1, x_2(0) = 0.1, \dot{x}_2(0) = 0$.
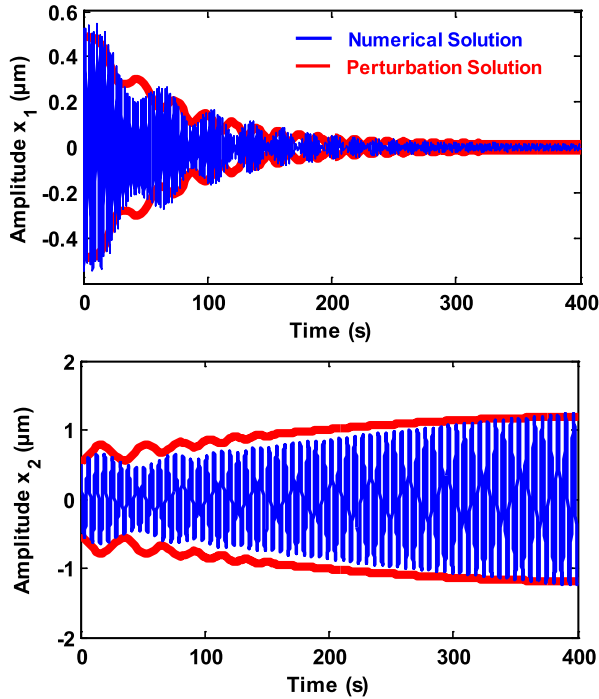
FIGURE 9. Comparison of the numerical solution with the analytical solution of the system before control at $\beta_1 = 5$, $\beta_2 = 0.4$ and $x_1(0) = 0.5$, $\dot{x}_1(0) = 0.5$, $x_2(0) = 0.5$, $\dot{x}_2(0) = 0$.
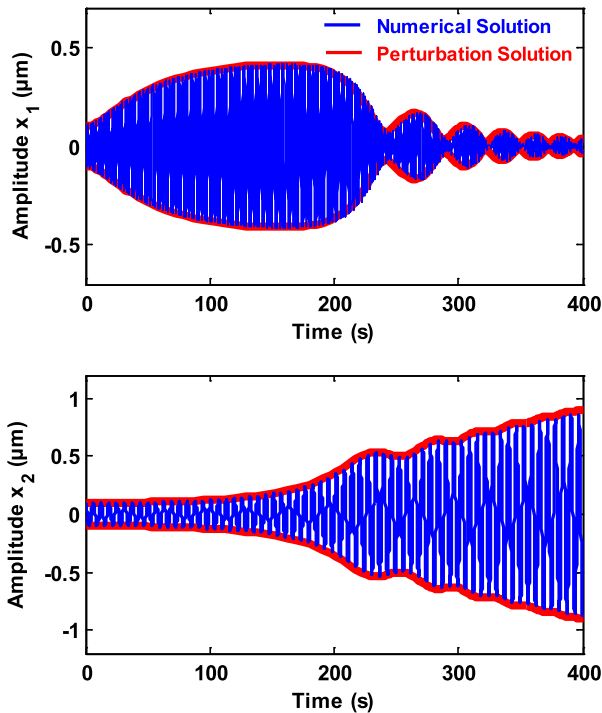

FIGURE 10. Comparison of the numerical solution with the analytical solution of the system after control at $\beta_1 = 5$, $\beta_2 = 0.4$ and $x_1(0) = 0.1$, $\dot{x}_1(0) = 0.1$, $x_2(0) = 0.1$, $\dot{x}_2(0) = 0$.

C. EFFECT OF SOME DIFFERENT PARAMETERS ON THE SYSTEM BEFORE AND AFTER CONTROL

The effect of some different parameters on the system response before and after control was studied at $\sigma_1 = 0$.

The blue and black solid line refer to the perturbation solution before and after control, while the red solid line refer to the numerical solution. Figures 7(a, b, c) show that the system behavior is increasing function in the excitation force f_1 and decreasing function in the control parameters β_1 and the damping coefficient ζ_1. With these figures, the system oscillations are eliminated before and after control using these parameters.

D. COMPARISON BETWEEN THE NUMERICAL AND ANALYTICAL SIMULATION

In figures 8, 9 and 10, we compare the numerical simulation of the system equations (1) and (2) with the perturbation solution of equations (29)-(32) before and after control at different values of control coefficients β_1, β_2 and initial conditions $x_1(0)$, $\dot{x}_1(0)$, $x_2(0)$, $\dot{x}_2(0)$. By change the initial conditions for the system, the oscillation response begins with increasing amplitude and becomes stable with chaotic motion as in figure 9, and tuned motion as in figure 10. The blue solid line refer to the numerical integration, while the red solid line refer to the perturbation (analytical) solution. We found a good agreement between the two solutions.

V. CONCLUSION

Active vibration control is a widely applied method for controlling helicopter vibration. Due to the great advances in microelectronics, this technology is superior to traditional control methods. Helicopter vibration has been a problem since the early days of helicopter development, and it has a direct effect on production and maintenance costs. In this research, an active vibration control to mitigate the oscillations of helicopter blade flapping system with harmonic and parametric excitations was investigated. The approximate solutions were calculated using the multiple scale perturbation technique. Furthermore, the stability, bifurcation analysis, numerical simulations for the vibrating system were studied. Comparison of the analytical with numerical solutions is obtained. This study included the following:

- After control, the helicopter blade suffered severe vibrations and jumps due to the presence of bifurcation points.
- The efficiency of the controller E_a was about **40**, means that the controller reduced the vibrations of the system by about **97.55%** from its value before controllers.
- The system response is decreasing the linear damping coefficient ζ_1 and natural frequencies ω_1 and ω_2.
- The system response is increasing with increasing the damping coefficient ζ_2, the non-linear parameter α_1 and the excitation amplitudes $f_j(j = 1, 2, 3)$.
- The jump phenomena and multivalued solutions are appeared with the positive and negative values of the nonlinear parameters β_1.
- With increasing values of the nonlinear parameters β_2, the system response is decreased and the curves are shifted to the left.

- The amplitude of the controller is increasing with increasing the damping coefficient ζ_2 and decreasing with increasing the nonlinear parameters β_1.
- Figures (7-9) show that the verification curves presented a good degree of closeness between analytical predictions and numerical simulation.

APPENDIX

$$\Gamma_5 = \frac{f_2}{4\omega_1} \sin 2\theta_{10} - \omega_1 \zeta_1,$$

$$\Gamma_6 = \left(\frac{f_1}{2\omega_1} \cos \theta_{10} + \frac{a_0 f_2}{4\omega_1} \cos 2\theta_{10} - \frac{f_3}{4\omega_1} \sin \theta_{10} \right),$$

$$\Gamma_7 = \frac{\sigma}{a_0} - \frac{9\alpha_1 a_0}{8\omega_1} + \frac{f_2}{4\omega_1 a_0} \cos 2\theta_{10},$$

$$\Gamma_8 = -\frac{f_1}{2\omega_1 a_0} \sin \theta_{10} - \frac{f_2}{2\omega_1} \sin 2\theta_{10} - \frac{f_3}{4\omega_1 a_0} \cos \theta_{10},$$

$$\Gamma_9 = \frac{f_2}{4\omega_1} \sin 2\theta_{10} - \omega_1 \zeta_1,$$

$$\Gamma_{10} = \frac{f_1}{2\omega_1} \cos \theta_{10} + \frac{a_0 f_2}{2\omega_1} \cos 2\theta_{10} - \frac{f_3}{4\omega_1} \sin \theta_{10},$$

$$\Gamma_{11} = \frac{\sigma}{a_0} - \frac{9\alpha_1 a_0}{8\omega_1} + \frac{\omega_2^2 \beta_1 b_0^2}{4\omega_1 a_0} + \frac{f_2}{4\omega_1 a_0} \cos 2\theta_{10},$$

$$\Gamma_{12} = -\frac{f_1}{2\omega_1 a_0} \sin \theta_{10} - \frac{f_2}{2\omega_1} \sin 2\theta_{10} - \frac{f_3}{4\omega_1 a_0} \cos \theta_{10},$$

$$\Gamma_{13} = \frac{\omega_2^2 \beta_1 b_0}{2\omega_1}, \quad \Gamma_{14} = \frac{\omega_1 \beta_2 b_0^2}{8\omega_2} \cos \theta_{40},$$

$$\Gamma_{15} = -\omega_2 \zeta_2 + \frac{\omega_1 \beta_2 a_0 b_0}{4\omega_2} \cos \theta_{40},$$

$$\Gamma_{16} = -\frac{\omega_1 \beta_2 a_0 b_0^2}{8\omega_2} \sin \theta_{40}, \quad \Gamma_{17} = -\frac{\sigma_4}{a_0} + \frac{9\alpha_1 a_0}{8\omega_1}$$
$$- \frac{\omega_2^2 \beta_1 b_0^2}{4\omega_1 a_0} - \frac{f_2}{4a_0 \omega_1} \cos 2\theta_{10} - \frac{3\omega_1 \beta_2 b_0}{4\omega_2} \sin \theta_{40},$$

$$\Gamma_{18} = \frac{f_1}{2a_0 \omega_1} \sin \theta_{10} + \frac{f_2}{2\omega_1} \sin 2\theta_{10} + \frac{f_3}{4a_0 \omega_1} \cos \theta_{10},$$

$$\Gamma_{19} = -\frac{\omega_2^2 \beta_1 b_0}{2\omega_1} - \frac{3\omega_1 \beta_2 a_0}{8\omega_2} \sin \theta_{40},$$

$$\Gamma_{20} = -\frac{3\omega_1 \beta_2 a_0 b_0}{8\omega_2} \cos \theta_{40}, \quad r_5 = - [\Gamma_5 + \Gamma_8 + \Gamma_{11} + \Gamma_{15}],$$

$$r_6 = [\Gamma_5 \Gamma_8 + (\Gamma_5 + \Gamma_8)(\Gamma_{11} + \Gamma_{16}) + \Gamma_{11}\Gamma_{16} - \Gamma_{12}\Gamma_{15}$$
$$- \Gamma_6 \Gamma_7], \quad r_7 = (\Gamma_5 + \Gamma_8)(\Gamma_{12}\Gamma_{15} - \Gamma_{11}\Gamma_{16})$$
$$+ (\Gamma_6 \Gamma_7 - \Gamma_5 \Gamma_8)(\Gamma_{11} + \Gamma_{16}) - \Gamma_6 \Gamma_9 \Gamma_{10} - \Gamma_9 \Gamma_{14} \Gamma_{12},$$

$$r_8 = (\Gamma_5 \Gamma_8 - \Gamma_6 \Gamma_7)(\Gamma_{11} \Gamma_{16} - \Gamma_{12} \Gamma_{15})$$
$$+ \Gamma_6 \Gamma_9 (\Gamma_{10} \Gamma_{16} - \Gamma_{12} \Gamma_{15}) + \Gamma_5 \Gamma_9 \Gamma_{12} \Gamma_{14}$$

CONFLICTS OF INTEREST

The authors declare that there are no conflicts of interest associated with this publication.

ACKNOWLEDGMENT

REFERENCES

[1] P. F. Pai, B. Wen, A. S. Naser, and M. J. Schulz, "Structural vibration control using PZT patches and nonlinear phenomena," *J. Sound Vibrat.*, vol. 215, no. 2, pp. 273–296, Aug. 1998.

[2] D. Kunz, "Saturation control for suppressing helicopter blade flapping vibrations—A feasibility study," in *Proc. 39th AIAA/ASME/ASCE/AHS/ASC Struct., Struct. Dyn., Mater. Conf. Exhib.*, Apr. 1998, pp. 1–7.

[3] H. W. Rong, X. D. Wang, W. Xu, and T. Fang, "Saturation and resonance of nonlinear system under bounded noise excitation," *J. Sound Vibrat.*, vol. 291, nos. 1–2, pp. 48–59, Mar. 2006.

[4] M. Eissa, W. A. A. El-Ganaini, and Y. S. Hamed, "Saturation, stability and resonance of non-linear systems," *Phys. A, Stat. Mech. Appl.*, vol. 356, nos. 2–4, pp. 341–358, Oct. 2005.

[5] L. Jun, H. Hongxing, and S. Rongying, "Saturation-based active absorber for a non-linear plant to a principal external excitation," *Mech. Syst. Signal Process.*, vol. 21, no. 3, pp. 1489–1498, Apr. 2007.

[6] L. Jun, L. Xiaobin, and H. Hongxing, "Active nonlinear saturation-based control for suppressing the free vibration of a self-excited plant," *Commun. Nonlinear Sci. Numer. Simul.*, vol. 15, no. 4, pp. 1071–1079, Apr. 2010.

[7] W. A. A. El-Ganaini, M. M. Kamel, and Y. S. Hamed, "Vibration reduction in ultrasonic machine to external and tuned excitation forces," *Appl. Math. Model.*, vol. 33, no. 6, pp. 2853–2863, Jun. 2009.

[8] M. M. Kamel, W. A. A. El-Ganaini, and Y. S. Hamed, "Vibration suppression in ultrasonic machining described by non-linear differential equations," *J. Mech. Sci. Technol.*, vol. 23, no. 8, pp. 2038–2050, Aug. 2009.

[9] M. M. Kamel, W. A. A. El-Ganaini, and Y. S. Hamed, "Vibration suppression in multi-tool ultrasonic machining to multi-external and parametric excitations," *Acta Mechanica Sinica*, vol. 25, no. 3, pp. 403–415, Jun. 2009.

[10] M. M. Kamel and Y. S. Hamed, "Nonlinear analysis of an elastic cable under harmonic excitation," *Acta Mechanica*, vol. 214, nos. 3–4, pp. 315–325, Nov. 2010.

[11] Y. S. Hamed, M. Sayed, D. . .-X. Cao, and W. Zhang, "Nonlinear study of the dynamic behavior of a string-beam coupled system under combined excitations," *Acta Mechanica Sinica*, vol. 27, no. 6, pp. 1034–1051, Dec. 2011.

[12] M. Sayed and Y. S. Hamed, "Stability and response of a nonlinear coupled pitch-roll ship model under parametric and harmonic excitations," *Nonlinear Dyn.*, vol. 64, no. 3, pp. 207–220, May 2011.

[13] M. Sayed and M. Kamel, "Stability study and control of helicopter blade flapping vibrations," *Appl. Math. Model.*, vol. 35, no. 6, pp. 2820–2837, Jun. 2011.

[14] M. Sayed and M. Kamel, "1:2 and 1:3 internal resonance active absorber for non-linear vibrating system," *Appl. Math. Model.*, vol. 36, no. 1, pp. 310–332, Jan. 2012.

[15] Y. S. Hamed and Y. A. Amer, "Nonlinear saturation controller for vibration supersession of a nonlinear composite beam," *J. Mech. Sci. Technol.*, vol. 28, no. 8, pp. 2987–3002, Aug. 2014.

[16] A. T. El-Sayed and H. S. Bauomy, "Vibration control of helicopter blade flapping via time-delay absorber," *Meccanica*, vol. 49, no. 3, pp. 587–600, Mar. 2014.

[17] O. Perdomo and F.-S. Wei, "On the flapping motion of a helicopter blade," *Appl. Math. Model.*, vol. 46, pp. 299–311, Jun. 2017.

[18] A. Castillo Pardo, I. Goulos, and V. Pachidis, "Modelling and analysis of coupled flap-lag-torsion vibration characteristics helicopter rotor blades," *Proc. Inst. Mech. Eng., G, J. Aerosp. Eng.*, vol. 231, no. 10, pp. 1804–1823, Aug. 2017.

[19] S. Castillo-Rivera and M. Tomas-Rodriguez, "Helicopter flap/lag energy exchange study," *Nonlinear Dyn.*, vol. 88, no. 4, pp. 2933–2946, Jun. 2017.

[20] S. Castillo-Rivera and M. Tomas-Rodriguez, "Helicopter modelling and study of the accelerated rotor," *Adv. Eng. Softw.*, vol. 115, pp. 52–65, Jan. 2018.

[21] D. Adair and M. Jaeger, "Efficient calculation of hingeless rotor blade flap-lag-torsion dynamics for helicopters," in *Proc. AIAA Scitech Forum*, San Diego, CA, USA, Jan. 2019, pp. 7–11.

[22] N. Pnevmatikos, "Pole placement algorithm for control of civil structures subjected to earthquake excitation," *J. Appl. Comput. Mech.*, vol. 3, no. 1, pp. 25–36, 2017.

[23] U. Gabbert, F. Duvigneau, and S. Ringwelski, "Noise control of vehicle drive systems," *Facta Universitatis, Ser., Mech. Eng.*, vol. 15, no. 2, p. 183, Aug. 2017.

[24] D. Marinković, G. Rama, and M. Zehn, "Abaqus implementation of a corotational piezoelectric 3-node shell element with drilling degree of freedom," *Facta Universitatis, Ser., Mech. Eng.*, vol. 17, no. 2, p. 269, Jul. 2019.

[25] Y. S. Hamed, A. T. EL-Sayed, and E. R. El-Zahar, "On controlling the vibrations and energy transfer in MEMS gyroscope system with simultaneous resonance," *Nonlinear Dyn.*, vol. 83, no. 3, pp. 1687–1704, Feb. 2016.

[26] Y. S. Hamed, M. R. Alharthi, and H. K. AlKhathami, "Nonlinear vibration behavior and resonance of a Cartesian manipulator system carrying an intermediate end effector," *Nonlinear Dyn.*, vol. 91, no. 3, pp. 1429–1442, Feb. 2018.

[27] Y. S. Hamed, M. Sayed, and A. A. Alshehri, "Active vibration suppression of a nonlinear electromechanical oscillator system with simultaneous resonance," *J. Vibroeng.*, vol. 20, no. 1, pp. 42–61, Feb. 2018.

[28] Y. S. Hamed, A. El Shehry, and M. Sayed, "Nonlinear modified positive position feedback control of cantilever beam system carrying an intermediate lumped mass," *Alexandria Eng. J.*, vol. 59, no. 5, pp. 3847–3862, Oct. 2020.

[29] Y. Hamed, A. A. Aly, B. Saleh, A. F. Alogla, A. M. Aljuaid, and M. M. Alharthi, "Nonlinear structural control analysis of an offshore wind turbine tower system," *Processes*, vol. 8, no. 1, p. 22, Dec. 2019.

[30] Y. S. Hamed, H. Alotaibi, and E. R. El-Zahar, "Nonlinear vibrations analysis and dynamic responses of a vertical conveyor system controlled by a proportional derivative controller," *IEEE Access*, vol. 8, pp. 119082–119093, 2020.

[31] M. P. Cartmell, *Introduction to Linear, Parametric and Nonlinear Vibrations*. London, U.K.: Chapman & Hall, 1990.

[32] A. H. Nayfeh and B. Balachandran, *Applied Nonlinear Dynamics: Analytical, Computational and Experimental Methods*. New York, NY, USA: Wiley, 1995.

[33] A. H. Nayfeh, *Problems in Perturbation*. New York, NY, USA: Wiley, 1985.

[34] A. H. Nayfeh and D. T. Mook, *Nonlinear Oscillations*. New York, NY, USA: Wiley, 1995.

HANAN K. ALKHATHAMI received the M.Sc. degree in mathematics from Taif University, in 2017. Since 2017, she has been an Assistant Professor of mathematics with the Department of Mathematics, Faculty of Science and Home Economic, Bisha University, Saudi Arabia. Her research interests include modeling, dynamical systems, and the numerical and analytical computational methods for solving differential equations.

E. R. EL-ZAHAR received the M.Sc. and Ph.D. degrees in engineering mathematics from Menofia University, Egypt, in 2004 and 2008, respectively. He is currently a Full Professor of engineering mathematics with the Department of Mathematics, Prince Sattam Bin Abdulaziz University. He is the author of more than 70 scientific papers and two textbooks in refereed journals and international conferences. His research interests include theory of differential equations and its application, numerical analysis, modeling, numerical and semi-analytical and computational methods for solving differential equations, and engineering systems.

• • •

Y. S. HAMED received the M.Sc. and Ph.D. degrees in mathematics from the Faculty of Science, Menoufia University, Egypt, in 2005 and 2009, respectively. He is currently an Associate Professor of engineering mathematics with the Department of Physics and Engineering Mathematics, Faculty of Electronic Engineering, Menoufia University. Since 2009, he has been an Associate Professor of mathematics with the Department of Mathematics and Statistics, Taif University, Saudi Arabia. He has supervised and examined some of M.Sc. and Ph.D. degree students. His research interests include theory of differential equations and its application, numerical analysis, modeling, dynamical systems control, chaotic systems, renewable energy systems, vibration control and computational methods for solving differential equations, and engineering systems. He is also the Editor of *International Journal of Control, Automation and Systems* (IJCAS).